Simultaneous Design Optimization of Semi-Rigid Plane Steel Frames with Semi-Rigid Bases Using Bees and Genetic Algorithms

Osman Shallan[#1], Hassan M. Maaly[#2], Osman Hamdy[#3]

[#] Department of Structural Engineering, University of Zagazig, Zagazig, Egypt
[1]Professor and Head of Structural Department, E-mail: Osmanshalan@yahoo.com
[2]Associate Professor, E-mail: Dr.H.Maaly6@gmail.com
[3] Corresponding author, Ph.D. Student, E-mail: Osmanhmdy@gmail.com

***Abstract*—This paper performs a simultaneous cross-sections and semi-rigid connections optimization for plane steel frames with semi-rigid beam-to-column connections, in company with fixed, semi-rigid and hinged base connections using, for the first time, a bees algorithm (BA), along with a genetic algorithm (GA). Both of algorithms are applied using Shallan et al. [1]optimization model. In this paper, the truthful Kanvinde and Grilli[2]nonlinear model is used for simulating semi-rigid base connections, where this model considers all deformations in different base connection elements under the applied loads to determine the relative spring rotation θ_r for the sake of getting accurate base rotational stiffness value. In addition, Frye and Morris [3]nonlinear model is used for simulating semi-rigid beam-to-column connections. The P-Δ effect and geometric nonlinearity are considered. The stress and displacement constraints of AISC-LRFD [4] specifications, alongside size adjustment constraints, are considered in the design process.**

Keywords -Genetic algorithm; bees algorithm; plane steel frame; optimization; semi-rigid connection; geometrically nonlinear; the P-Δ effect; semi-rigid base.

I. INTRODUCTION

Most of the design procedures shorten the simulation of steel connections by assuming them either a perfectly pinned or a fully rigid connection. In opposition, actual steel connections have some rotational stiffness between these two severe assumptions, and their real behavior is complicated and nonlinear. Thus, for a precise structural analysis, a nonlinear model is required for simulating steel connections either beam-to-column connections or base connections, along with considering the P-Δ effect and geometric nonlinearity (i.e., the change in coordination).

Two types of steel constructions are termed in AISC-LRFD[4]: fully restrained (FR) and partially restrained (PR), where the PR type is considered according to rational experimental and numerical studies.

Some researchers worked on the behavior of semi-rigid connections using experimental studies to get the nonlinear behavior of the connection such as Frye and Morris[3], Abdalla and Chen[5], Chisala[6], Kim et al. [7], Wu et al. [8], Aydin et al. [9]and Maali et al. [10]. Due to its rational simulation and it's wide usage in the literature studies, the odd-polynomial Frye and Morris [3]model are used in the current study. On the contrary of beam-to-column connections, an accurate model of semi-rigid base connections is usually unnoticed in most of the literature studies. Only Kanvinde and Grilli[2]model is reasonably accurate for modeling semi-rigid base connection, where it considers deformations of all different elements of the base connection, so this model is used in the current study to simulate base connections.

BA is one of the evolutionary population-based optimization algorithms, which simulates the natural foraging behavior of honey bees to discover the best solution to get a honey.Furthermore; GA is one of the first evolutionary population-based optimization algorithms, which imitates the evolution theory of Darwin.

II. SUMMARY OF THE LITERATURE STUDIES

Table 1 shows a comparison between the previous literature studies, where all the literature studies simulate the beam-to-column connection using Frye and Morris [3]model, while Hensman and Nethercot[11]model is used to simulate the base connection if it is considered as a semi-rigid.

Table 1 Comparison between previous studies

Study	Frame	Base	Used algorithm	Design code
Shallan*et al.*[1]	Plane	Fixed	TLBO, GA	AISC-LRFD
Musa and Ayse[12]	Space	Fixed	GA	AISC-LRFD
Musa Artar[13][a]	Plane	Fixed	TLBO	AISC-ASD
Musa and Ayse[14]	Plane	Semi-rigid	GA	AISC-ASD
Musa and Ayse[15][b]	Plane	Fixed	GA	AISC-LRFD
Musa and Ayse[16][b]	Space	Fixed	GA	AISC-LRFD
Hadidi and Rafiee[17]	Plane	Fixed	New HS	AISC-LRFD
Mohammad and Payam[18]	Plane	Fixed	Fuzzy GA	AISC-ASD
Alqedra *et al.*[19]	Plane	Fixed	ITHS	AISC-LRFD
Arafa *et al.*[20]	Plane	Fixed	HS	AISC-LRFD
Hadidi and Rafiee[21]	Plane	Fixed	Improved PSO	AISC-LRFD
Rafiee and Hadidi[22]	Plane	Fixed	BB-BC	AISC-LRFD
Hayalioglu and Degertekin[23]	Plane	Semi-rigid	HS	AISC- LRFD
Hayalioglu and Degertekin[24]	Plane	Semi-rigid	GA	AISC-LRFD
Hayalioglu and Degertekin[25]	Plane	Fixed	GA	AISC-ASD
Degertekin and Hayalioglu[26]	Plane	Semi-rigid	GA	Turkish code

[a]Braced frame, [b] Composite beam, ITHS: Intelligent tuned harmony search, TLBO: Teaching-learning-based optimization, HS: Harmony search,PSO: Particle swarm optimization, BB-BC: Big bang-big crunch.

III. GENETIC ALGORITHM (GA)

A genetic algorithm is one of the oldest optimization algorithms inspired by John Holland [27], where it mimics the evolution theory of Darwin. GA starts with an initial population consists of a certain number of listed suggested solutions, where each solution is called individual or chromosome.

Each individual or chromosome consists of a string of genes, where each gene represents a certain suggested optimization variable. These genes are coded in a binary-string, so decoding process is proceeded to convert genes to decimal values, then the fitness value of the problem using these suggested variables is determined for each individual in the initial population.

Based on the fitness value of each individual, the selection process is carried out to select chosen individuals to go through a reproduction process. Crossover and mutation are the main reproduction parameters used for creating the next generation of solutions, by repeating the same steps until reaching the last generation. Fig. 1 shows a flowchart of GA processes.

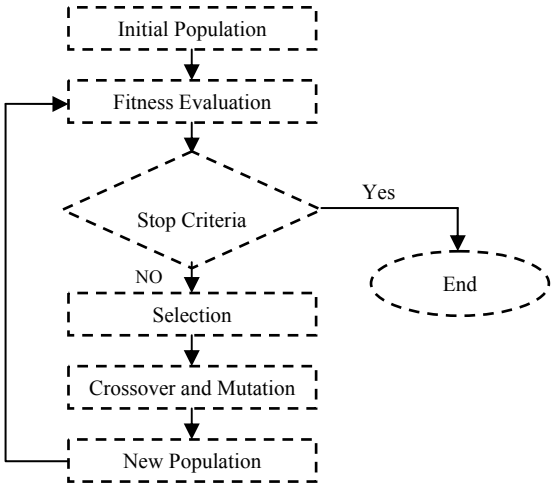

Fig. 1 Flowchart of the basic GA

IV. BEES ALGORITHM (BA)

The BA is an optimization algorithm inspired by Pham [28], it mimics the natural foraging behavior of honey bees to find the best solution.

The following is a description of the BA steps, while its flowchart is shown in Fig. 2.

1- The algorithm starts with the (n) scout bees being located randomly in the search space, these bees represent the initial population, for example, n=10 as shown in Figs. 3 and 4.

2- The fitness of the sites visited by the scout bees after the return are evaluated and sorted in a descending order and stored in an array.

3- The best m sites will be selected out of (n), and then we choose the best e site out of (m), for example, m=5, and e=2 as shown in Fig. 5.

4- Recruit the number of bees for the selected sites and evaluate the fitness of the sites as follows:

A number of bees (n_2) will be selected randomly to be sent to e sites and choosing (n_1) bees randomly which their number is less than n_2, to be sent to m-e sites.

5- A neighborhood search sites of a size (ngh) is selected, where ngh will be used to update the m bees declared in the previous step if there is any better neighbor solution as shown in Figs. 6,7 and 8.

6- Choosing the best m bee (the highest fitness) to the next bee generation where other bees in the generation will be assigned randomly around the search space (n-m) as shown in Fig. 9.

7- Steps from 1 to 5 are repeated till reaching the last generation and get the optimum solution as shown in Fig. 10.

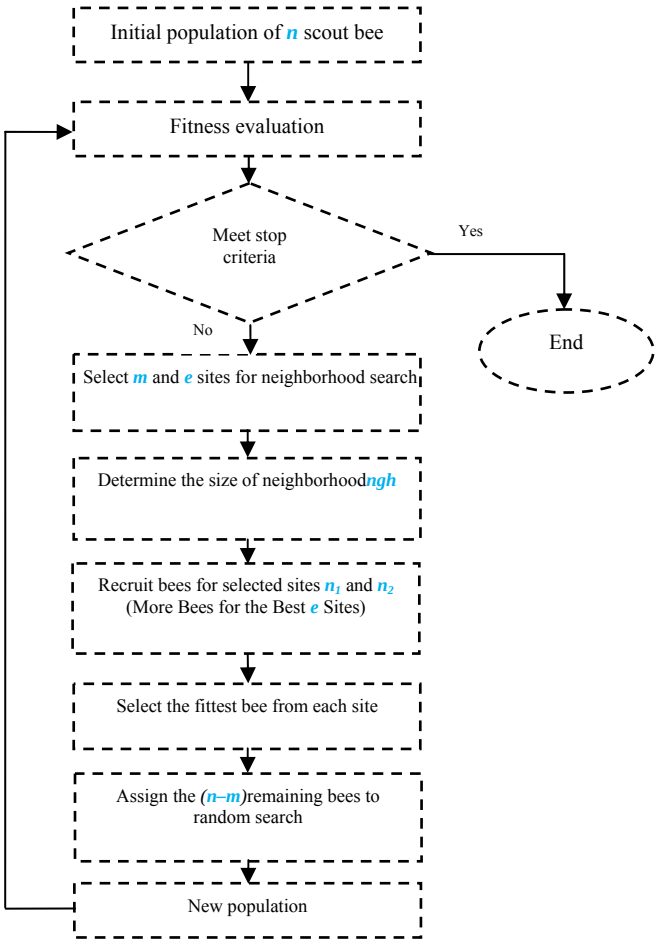

Fig. 2 Flowchart of the basic BA

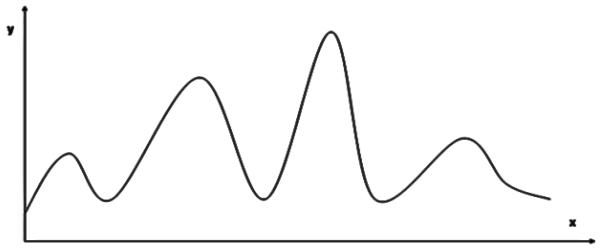

Fig. 3 Area of search, where highest location needed to be found

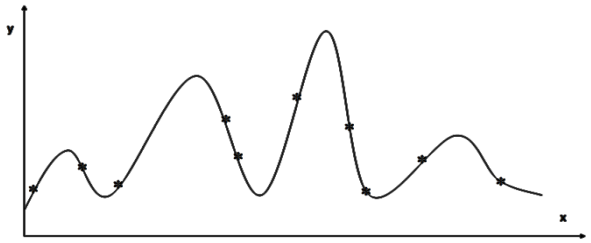

Fig. 4 Initialize a population of (n=10) scout bees with random search and evaluate the fitness

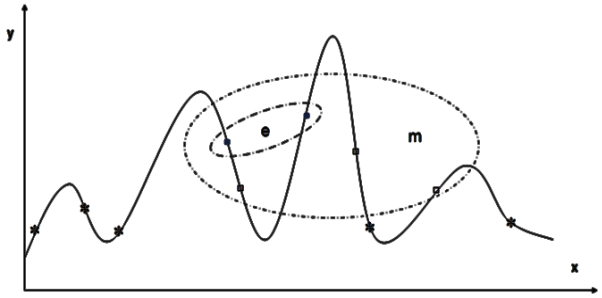

Fig. 5 Select (m=5) for best bees, and (e=2) for elite bees and (m-e=3) other selected bees

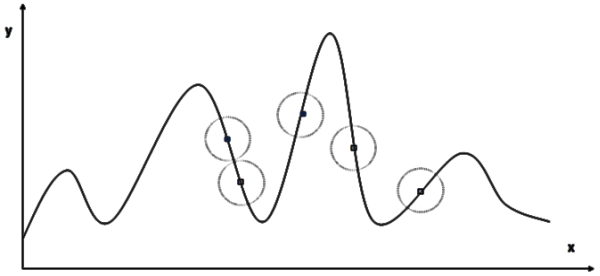

Fig. 6 Determine the size of neighborhood size (ngh)

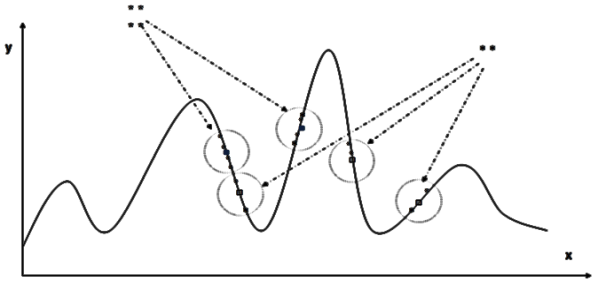

Fig. 7 Recruit bees for selected sites (more bees for the e=2 elite sites)

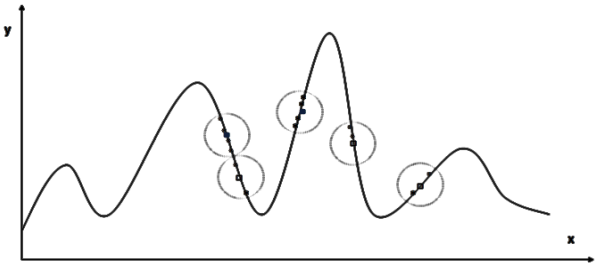

Fig. 8 Select the fittest bee from each site

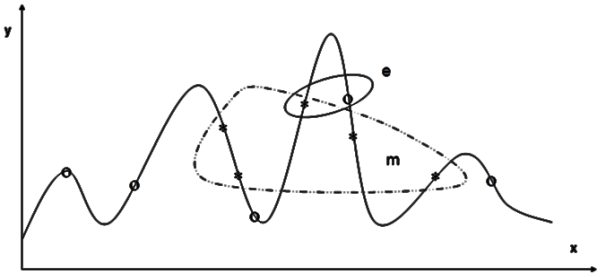

Fig. 9 Assign the (n–m) remaining bees to random search

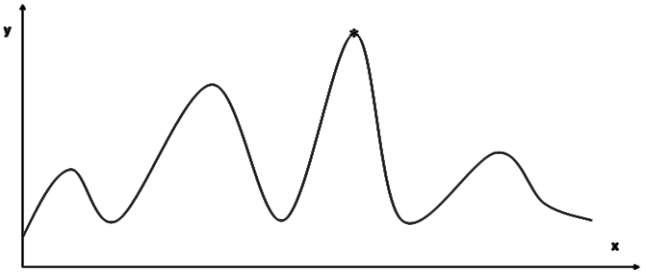

Fig. 10 Find the global best point

V. MODELING OF A SEMI-RIGID BASE CONNECTION

Hayalioglu and Degertekin[23], [24],[26] performed an optimization for a semi-rigid steel frame with a semi-rigid base, but they used Hensman and Nethercot[11] model to determine stiffnessK_{base} of four bolt flexible base as shown in Eqs. 1 and 2. This model is a linear-constant model and doesn't mimic the actual nonlinear behavior of the flexible base, and doesn't study deformations in different base connection elements, also it doesn't take consider the applied loads on the base connection.

$$K_{base} = \frac{E \times Z^2 \times t}{20} \quad (1)$$

$$Z = r_b + \frac{H_c}{2} - \frac{t_f}{2} \quad (2)$$

where E is the modulus of elasticity, t, r_b, H_c, and t_f are shown in Fig. 11.

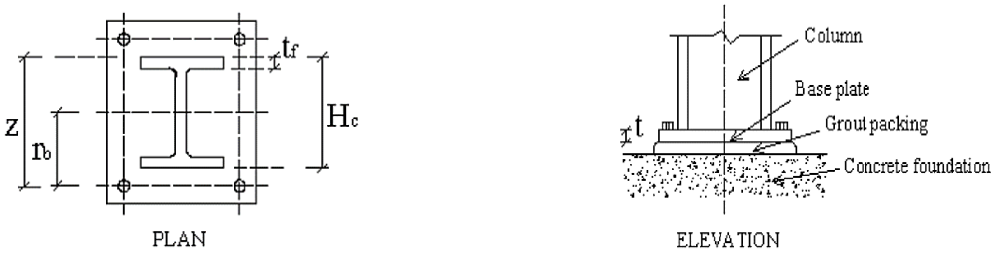

Fig. 11 simple semi-rigid column base detail using Hensman and Nethercot[11] model

The current study uses Kanvinde and Grilli[2] model to simulate the semi-rigid base connection, opposing to Hensman and Nethercot[11] model, this model is a nonlinear model, where it takes into the account the deformations in the different base elements, such as anchors, the concrete footing and base plate flap deformations in both tension and compression sides, based on the applied axial load P and moment M values. Kanvinde model is separated into two cases according to the eccentricity value e and the critical eccentricity value e_{crit}.

$$e = \frac{M}{P} \tag{3}$$

$$e_{crit} = \frac{N}{2} - \frac{P}{2 \times B \times f_{\max}} \tag{4}$$

$$f_{\max} = 0.85 \times f_c \times \left(\sqrt{\frac{A_2}{A_1}} \right) \leq 1.7 f_c \tag{5}$$

where N is the length of the base plate, B is the width of the base plate, f_c is the compressive strength of concrete under the base plate, f_{max} is the maximum bearing stress under the base plate for the bigeccentricity case as shown in Fig. 12 (b), A_1 is the bearing area of the base plate, and A_2 is the effective concrete area under the base plate.

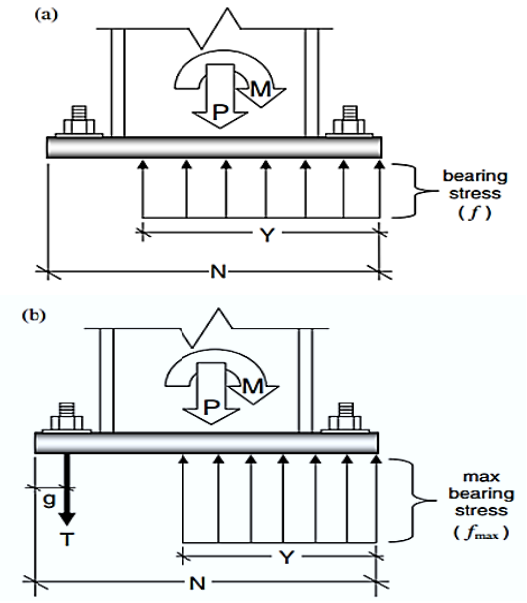

Fig. 12 Stress distributions assumed in current U.S. design practice for
(a) low; and (b) high-eccentricity conditions Kanvinde and Grilli[2]

A- Case 1, low eccentricity case

In this case, e $<e_{crit}$, and the spring rotation θ_r of the base connection is produced only by concrete strain at the edge of the base plate $\varepsilon_{conc.}^{toe}$ and concrete strain at the centerline of anchor rods onthe other side$\varepsilon_{conc.}^{rod}$.under bearing stress f with stress block length Y as shown in Fig. 12 (a).

$$f = \frac{P^2}{P \times B \times N - 2 \times M \times B} \tag{6}$$

$$Y = N - \frac{2 \times M}{P} \tag{7}$$

$$\varepsilon_{conc.}^{toe} = \frac{f}{E_{conc.}} \tag{8}$$

$$\varepsilon_{conc.}^{rod} = \varepsilon_{conc.}^{toe} \times \left(1 - \frac{M}{P \times e_{crit}}\right) \tag{9}$$

$$\theta_r = \frac{d \times \left(\varepsilon_{conc.}^{toe} - \varepsilon_{conc.}^{rod}\right)}{(S + N/2)} \tag{10}$$

where$E_{conc.}$ is the modulus of elasticity of concrete under the base plate which equals $E_{conc.} = 4700\sqrt{f_c}$ N/mm^2, d is the concrete footing depth, and $(S + N/2)$ is the distance between the edge of the base plate and the centerline of anchor rods in the other side as shown in Fig. 13.

B- Case 2, high eccentricity case

In this case, e >e_{crit} and the spring rotation θ_r of the base connection is produced by anchor strainΔ_{rod} Due to a tensile force, concrete stain $\Delta_{conc.}$ and plate flap deformation on the compression side $\Delta_{comp.}$ and tension sides $\Delta_{ten.}$under bearing stress f_{max} with stress block length Y as shown in Fig. 12 (b).

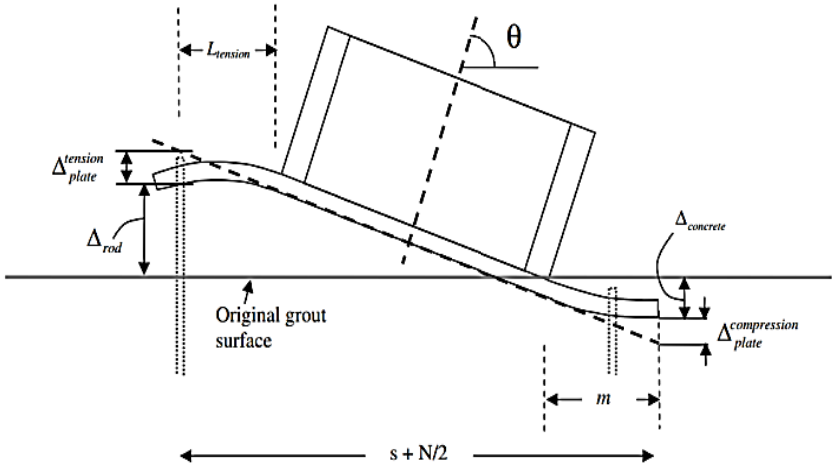

Fig. 13 Assumed deformation mode and contribution of various components Kanvinde and Grilli[2]

❖ *Anchor rod deformation* Δ_{rod}

$$\Delta_{rod} = \frac{T_{rod} \times L_{rod}}{A_{rod} \times E_{rod}} \tag{11}$$

$$T_{rod} = \frac{f_{\max} \times B \times Y - P}{N_{rod}} \tag{12}$$

$$Y = (N - g) - \sqrt{(N - g)^2 - \frac{2 \times [M + P \times (N/2 - g)]}{f_{\max} \times B}} \tag{13}$$

where g is shown in Fig. 12 (b), T_{rod} is the tension force in one rod, N_{rod} is the number of the anchor rods on one side, A_{rod} is the cross section gross area of one anchor rod, L_{rod} is the total length of the anchor rod which equals to (8-24)×diameter of the anchor rod[2], and E_{rod} is the modulus of elasticity of the anchor rod.

❖ *Concrete deformation* $\Delta_{conc.}$

$$\Delta_{conc.} = d \times \frac{f_{\max}}{E_{conc.}} \tag{14}$$

❖ *Base plate flap deformation in tension side* $\Delta_{ten.}$

$$\Delta_{ten.} = \left(T_{rod} \times N_{rod} \times \frac{L_{tension}^3}{3 \times E_{plate} \times I_{plate}} \right) + \left(T_{rod} \times N_{rod} \times \frac{L_{tension}}{3 \times A_{plate}^s \times G_{plate}} \right) \quad (15)$$

$$I_{plate} = B \times \frac{t_p^3}{12} \quad (16)$$

$$A_{plate}^s = 5/6 \times B \times t_p \quad (17)$$

where $L_{tension}$ is shown in Fig. 13, E_{plate} is the modulus of elasticity of base plate, t_p is the base plate thickness, and G_{plate} is the shear modulus of the base plate equals 77.2 Gpa.

❖ *Base plate flap deformation in compression side* $\Delta_{comp.}$

If Y ≥ m

$$\Delta_{comp} = f_{\max} \times B \times \left(\frac{m^4}{8 \times E_{plate} \times I_{plate}} + \frac{m^2}{2 \times A_{plate}^s \times G_{plate}} \right) \quad (18)$$

If Y < m

$$\Delta_{comp} = \frac{f_{\max} \times B}{8 \times E_{plate} \times I_{plate}} \times \left(m^4 - \frac{1}{3}(m-Y)^3 \times (3m+Y) \right) + \frac{f_{\max} \times B \times Y}{A_{plate}^s \times G_{plate}} \times \left(m - Y + \frac{Y^2}{2} \right) \quad (19)$$

where m is the flap length of the base plate as shown in Fig. 13.

Finally, a spring rotation θ_r of the base connection can be calculated as follows.

$$\theta_r = \frac{\left(\Delta_{rod} + \Delta_{conc.} + \Delta_{ten.} + \Delta_{comp.} \right)}{\left(S + N/2 \right)} \quad (20)$$

For simplification, some dimensions are considered fixed during the design optimization procedure such as rod gross diameter=2.5 cm, L_{rod}=50 cm, d =120 cm, N_{rod}=2, t_p=2.5 cm, and the base plate extension out of column section=10 cm for each side, where the anchor bolts at 5 cm of column flange edge, the pedestal extension out of the base plate=10 cm for each side.

VI. MODELING OF A SEMI-RIGID BEAM-TO-COLUMN CONNECTION

Similar to the literature studies, Frye and Morris [3]model is assumed in the current study because it is easy to apply and it is an odd-power polynomial model, which is reasonably worthy for simulation of the nonlinear M-$\boldsymbol{\theta_r}$behavior of the semi-rigid beam-to-column connections, as expressed in the following equation.

$$\theta_r = C_1(\kappa M)^1 + C_2(\kappa M)^3 + C_3(\kappa M)^5 \quad (21)$$

where C_1, C_2, and C_3 are the curve-fitting constants, and$\boldsymbol{\kappa}$is a standardization constant dependent on the connection type and geometry, as shown in Table 2 [29].

Fig. 14 shows that Frye and Morris's model is valid to eight different types of the semi-rigid beam-to-column connections.

According to the literature studies [21], [17] and others, and to simplify the problem, some of the connection size parameters required in Frye-Morris polynomial model [3] are taken fixed through the design optimization procedure, as shown in Table 3. Moreover, for connections 1, 2, and 8, d_a&d_p=web depth-10.16 cm, also, for connections 5 and 6, d_g=beam depth+15.24 cm[1].

Table 2 The curve-fitting constants

Connection type	Curve-fitting constants			Standardization parameter (κ)
	C_1	C_2	C_3	
1	4.28×10^{-3}	1.45×10^{-9}	1.51×10^{-16}	$\kappa = d_a^{-2.4} t_a^{-1.81} g^{0.15}$
2	3.66×10^{-4}	1.15×10^{-6}	4.57×10^{-8}	$\kappa = d_a^{-2.4} t_a^{-1.81} g^{0.15}$
3	2.23×10^{-5}	1.85×10^{-8}	3.19×10^{-12}	$\kappa = d^{-1.287} t^{-1.128} t_c^{-0.415} \ell_a^{-0.694} g^{1.35}$
4	8.46×10^{-4}	1.01×10^{-4}	1.24×10^{-8}	$\kappa = d^{-1.5} t^{-0.5} \ell_a^{-0.7} d_b^{-1.5}$
5	1.83×10^{-3}	1.04×10^{-4}	6.38×10^{-6}	$\kappa = d_g^{-2.4} t_p^{-0.4} d_b^{-1.5}$
6	1.79×10^{-3}	1.76×10^{-4}	2.04×10^{-4}	$\kappa = d_g^{-2.4} t_p^{-0.6}$
7	2.10×10^{-4}	6.20×10^{-6}	-7.60×10^{-9}	$\kappa = d^{-1.5} t^{-0.5} \ell_t^{-0.7} d_b^{-1.1}$
8	5.10×10^{-5}	6.20×10^{-10}	2.40×10^{-13}	$\kappa = d_p^{-2.3} t_p^{-1.6} t_w^{-0.5} g^{1.6}$

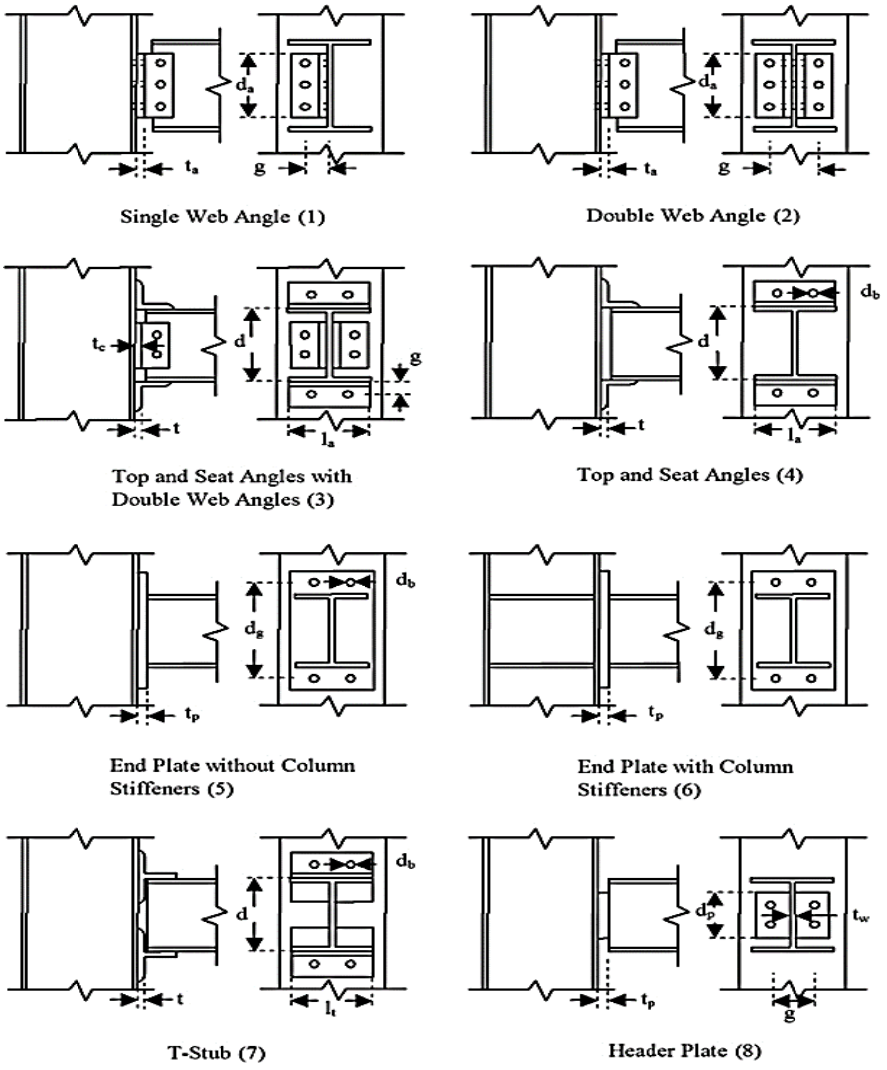

Fig. 14 Semi-rigid beam-to-column connection types [17]

Connection type	Fixed connection size parameters (cm)	Values in Eq. 27 (kN·mm/rad)
1	$t_a = 2.54, g = 11.43$	85×10^6
2	$t_a = 2.858, g = 25.4$	113×10^6
3	$t = 2.54, t_c = 2.54, g = 11.43$	282×10^6
4	$t = 2.54, d_b = 2.858$	226×10^6
5	$t_p = 2.54, d_b = 2.858$	339×10^6
6	$t_p = 2.54$	395×10^6
7	$t = 3.81, d_b = 2.858$	452×10^6
8	$t_p = 2.54, g = 25.4$	141×10^6

VII. NONLINEAR ANALYSIS PROCESS

Similar to the literature studies, the displacement method is used to carry out the structural analysis process in the present study, wherein, the stiffness matrix of the frame is formed by gathering of the stiffness matrices of the different frame members in the global coordinates [29]. In order to take the P-Δ effects, in addition to the geometrical nonlinearity into account during the analysis process, an incremental approach is applied [30], such that, in each load increment the stiffness matrices are updated using the most recently calculated axial force values for column elements, besides, updating the frame geometry based on the most recently geometric deformations through an iterative process until the convergence is achieved [29].

Furthermore, the secant stiffness approach is applied to consider the nonlinearity of a semi-rigid connection of beam members and column members connected with a semi-rigid base.

Fig. 15 shows the connection secant stiffness values corresponding to all load increments, where Fig. 16 shows the moment-rotation curves of the eight connection types [29].

The convergence criterion for each set of iterations is measured by comparing the difference between the end forces of the members with the applied incremental loads so as to be smaller than a pre-determined tolerance.

A convergent result of a load increment establishes an initial estimation for the first iteration of the next load increment, and the iterative process continues until considering the final load increments. The results for all load increments are accumulated to determine the total nonlinear response of the semi-rigid frame.

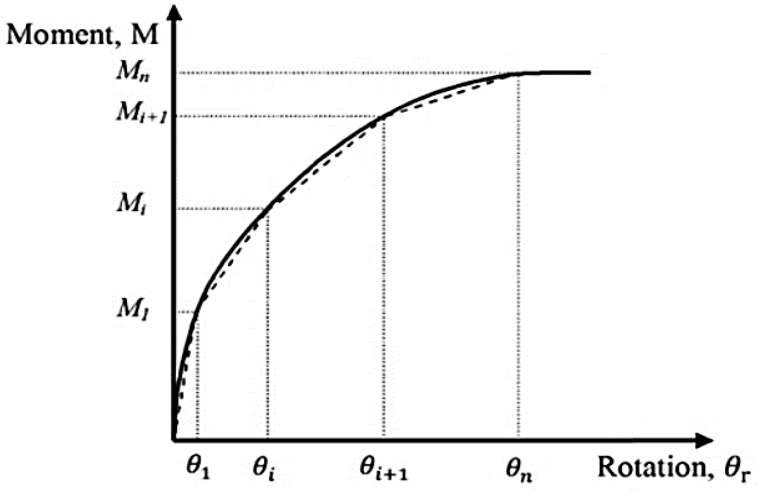

Fig. 15 Secant stiffness through the M-Θ_r curve [17]

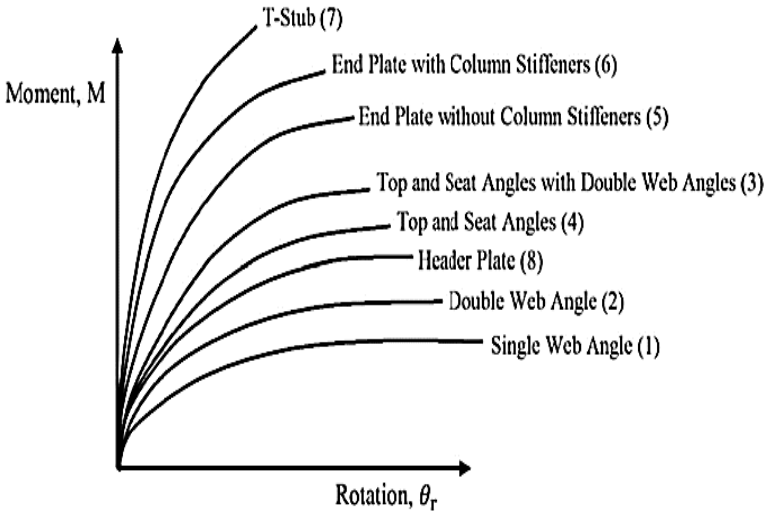

Fig. 16 Moment-Rotation curves of semi-rigid connection types [17]

VIII. DESIGN CONSTRAINTS

Design constraint check ensures that either the resulting frame is safe and serviceable or not. Following previous studies [29], [17] and others, the following constraints are used in the current study.

1- AISC-LRFD [4] strength constraint using the interaction equation of the bending moment and the axial force as follows:

$$\text{For } \frac{P_u}{\phi P_n} \geq 0.2 \qquad \left(\frac{P_u}{\phi P_n}\right) + \frac{8}{9}\left(\frac{M_{ux}}{\phi_b M_{nx}}\right) \leq 1 \tag{22}$$

$$\text{For } \frac{P_u}{\phi P_n} < 0.2 \qquad \frac{1}{2}\left(\frac{P_u}{\phi P_n}\right) + \left(\frac{M_{ux}}{\phi_b M_{nx}}\right) \leq 1 \tag{23}$$

where $\boldsymbol{P_u}$ $\boldsymbol{and}$ $\boldsymbol{P_n}$ are the required and the nominal strength of a member, respectively, either compression or tension, and $\emptyset$ is a reduction factor equal to 0.9 in the case of tension or compression. Moreover, $\boldsymbol{M_{ux}}$ $\boldsymbol{and}$ $\boldsymbol{M_{nx}}$ are the required and nominal flexural strength of a member about its major axis, respectively, where the ending reduction factor $\emptyset_{\boldsymbol{b}}$ equals 0.9.

Semi-rigidity of beam member ends are reflected in determining the restraint factor G and fixed end forces according to Dhillon and O'Malley III[29].

2- In addition, the roof drift and inter-story drift constraints are taken into account, where the allowable roof drift equals 0.0052×total frame height. Moreover, the allowable inter-story drift is controlled by story height/300.

3- For construction necessity, the size adjustment constraint is considered, firstly, this constraint makes certain that a beam flange is not wider than a column flange at all connections. In addition, a column depth in a higher floor is not bigger than the same column depth on a lower floor.

IX. DESIGN VARIABLES

According to the developed optimization model of Shallan et al. [1], the rotational deformation of a member ends Θ_A& Θ_B used as design variables to determine column inertia I_c or beam inertia I_B as follows.

$$I_c = Max\left(\frac{M_A - M_{FA} + \frac{6\Delta}{L^2}}{\frac{E}{L}\left[4\theta_A + 2\theta_B\right]}, \frac{M_B - M_{FB} + \frac{6\Delta}{L^2}}{\frac{E}{L}\left[4\theta_B + 2\theta_A\right]}\right) \tag{24}$$

$$I_b = Max\left(\frac{M_A - M_{FA}}{\frac{E}{L}\left[3.2\theta_A + 1.6\theta_B\right]}, \frac{M_B - M_{FB}}{\frac{E}{L}\left[3.2\theta_B + 1.6\theta_A\right]}\right) \tag{25}$$

where M_A&M_B is the preliminary moments for the same frame using any logical sections and fixed connections, M_{FA}&$M_{FB}$are the fixed end moments, Δ is the allowable inter-story drift, E is the modulus of elasticity, and L is the member length.

X. TOTAL COST AND PENALIZATION

The total cost of a plane steel frame bearing in mind the cost of the members and the semi-rigid beam-to-column connections is defined by Xu and Grierson [31] as follows.

$$Total\_Cost = \sum_{i=1}^{NM} \gamma_s A_i L_i + \sum_{i=1}^{NB} \sum_{j=1}^{2} \left(\beta_{ij} R_{ij} + \beta_{ij}^0 \right) \tag{26}$$

$$\beta_{ij} = \frac{0.225 \gamma_s A_i L_i}{S_i} \tag{27}$$

$$\beta_{ij}^0 = 0.125 \gamma_s A_i L_i \tag{28}$$

where $\boldsymbol{\gamma_s}$ is the steel density, A_i is the cross-sectional area, L_i is the member length, $\boldsymbol{R_{ij}}$ is the rotational stiffness of the connection, j represents two ends of a semi-rigid connection, NM and NB represent the total number of members and beams in the frame, respectively, $\boldsymbol{S_i}$ is an estimated value for rotational stiffness of a connection, as shown in Table 3.

Penalty function gives a bad fitness value for any solution violates any constraint to terminate it as expressed in the following equation.

$$Fitness = Total\_\text{cost} + C \times 10^8 \tag{29}$$

where C is the penalty constant equals zero for the solutions achieve all constraints, otherwise, it equals one.

XI. NUMERICAL EXAMPLES

Three benchmark examples are examined in the current study to investigate the effect of simulating the semi-rigid base connection using Kanvinde model, whereas both BA and GA optimization techniques are used. Three base connection cases are considered in the current study; fixed (F), semi-rigid (S), and hinged (H). The used algorithms properties and steel properties are as follows.

Algorithms properties.

The algorithms used in the following benchmark examples are a genetic algorithm with reproduction parameters of 0.9 for the crossover and 0.05 for the mutation, in addition, a bees algorithm. Both of the algorithms have a population size of 100, and 50 maximum generations/iterations.

Steel properties.

A36 steel is used, where $\boldsymbol{E = 200\ Gpa}$, yield stress $\boldsymbol{f_y = 250\ Mpa}$, shear modulus $\boldsymbol{G = 77.2\ Gpa}$, and the unit weight of material $\boldsymbol{\gamma_s = 7.85\ t/m^2}$, according to AISC-LRFD[4].

11.1 Single bay with a nine-story frame.

The geometry of the single bay with a nine-story frame, along with the member grouping and the design loads are shown in Fig. 17. The W, W_1, and W_2 loads are equal to 17.8 kN, 27.14 kN/m, and 24.51 kN/m, respectively.

The member cross-sections and the story connections for the optimum solutions using BA and GA for the three base connection cases are shown in Tables 4 and 5, respectively.

It is obvious from the results and Fig. 16 that the most rigid connections, i.e., types 6 and 7 are mostly chosen.

Furthermore, a comparison between the total frame cost, weight and roof drift of the optimum frames in the current study with those in previous studies are shown in Table 6. The comparison shows that GA achieves a better result than BA for all base connection cases, while both of the algorithms achieve better results than the literature results using same base case, i.e., fixed base.

Figs. 18, 19, and 20 show the effect of different base connection cases on the roof drift, weight, and the total frame cost, correspondingly, where these figures show that there is no difference between F and S cases except minor increment in roof drift at S case, it indicates that the relative rotation of base connection is negligible and the applied loads produce insignificant deformation on different base component using Kanvinde model. On the other hand, H case obtains the highest cost, weight, and roof drift.

Table 4 Member sections of optimum frames

Mem. grouping no.	BA		GA	
	F and S	H	F and S	H
1	W24X68	W30X90	W24X68	W27X84
2	W24X55	W24X62	W24X55	W21X55
3	W18X35	W21X48	W18X35	W21X44
4	W24X68	W30X90	W24X68	W27X84
5	W24X55	W24X62	W24X55	W21X55
6	W18X35	W21X48	W18X35	W21X44
7	W18X35	W21X48	W16X31	W21X44

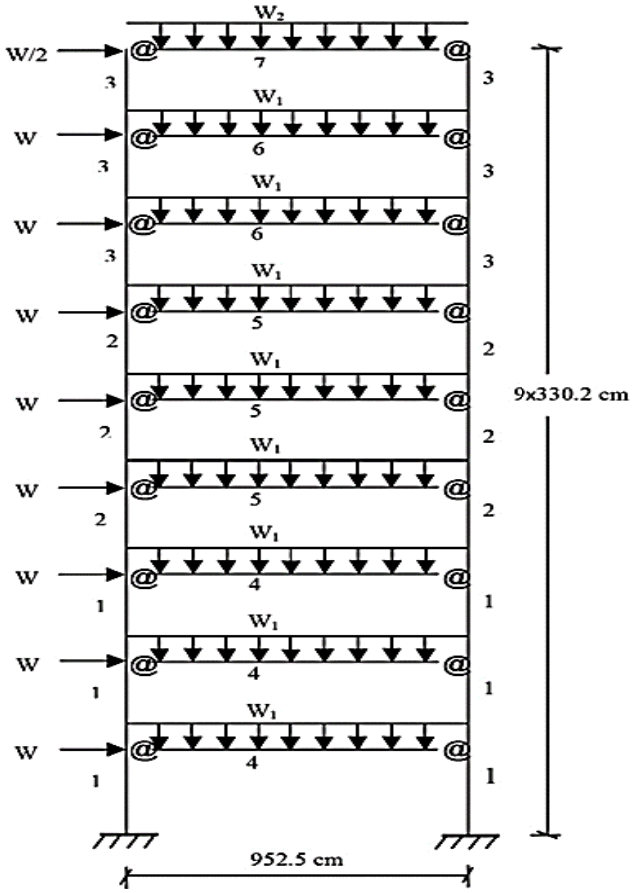

Fig. 17 Single bay with a nine-story frame[17].

Table 5 Story connections of optimum frames

Story no.	BA		GA	
	F and S	H	F and S	H
1	7	7	7	7
2	6	4	6	6
3	6	4	6	6
4	6	6	6	7
5	6	6	6	6
6	6	7	6	7
7	7	7	7	7
8	5	7	5	7
9	7	7	5	7

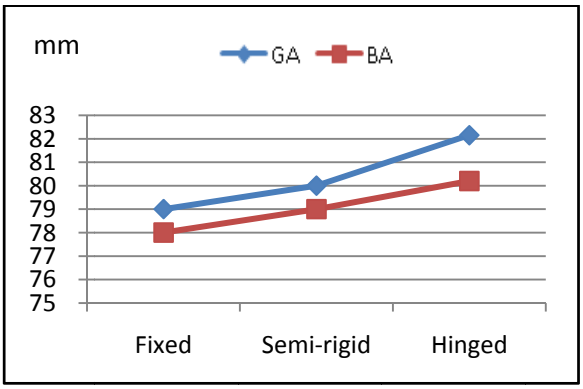

Fig.18 The roof drift usingBA and GA

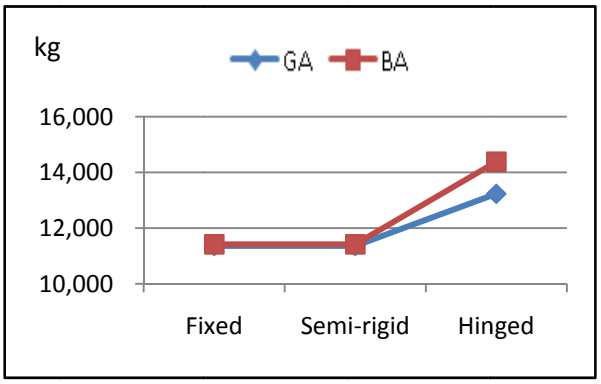

Fig.19 The total frame weight using BA and GA

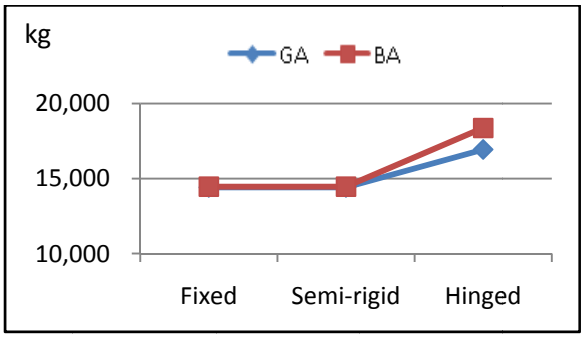

Fig. 20 The total frame cost using BA and GA

Table 6 Comparisons between the current study and previous works.

Study	Algorithm	Base case	Conn. type	T.s (mm)	W (kg)	T.C (kg)
Rafiee et al. [22]	BB-BC	F	1	56	38,718	40,520
		F	2	55	32,617	36,235
		F	3	66	14,809	16,881
		F	4	76	23,956	25,786
		F	5	54	30,804	33,488
		F	6	65	33,481	35,799
		F	7	44	43,450	53,601
		F	8	71	44,527	46,146
Hadidi and Rafiee[21]	HS-PSO	F	1	79	18,693	21,486
		F	2	73	13,182	17,886
		F	3	70	13,468	15,464
		F	4	71	14,288	16,499
		F	5	70	12,901	15,773
		F	6	69	12,136	14,970
		F	7	69	11,590	14,787
		F	8	73	19,722	21,757
Hadidi and Rafiee[17]	BB-BC	F	V	71	14,512	17,201
	HS	F	V	75	13,960	16,495
	HS-BB-BC	F	V	77	12,218	14,610
Shallan et al. [1]	TLBO	F	V	78	11,420	14,462
	GA	F	V	79	11,363	14,410

Current study	GA	S	V	80	11,363	14,410
		H	V	82	13,233	16,934
	BA	F	V	78	11,420	14,461
		S	V	79	11,420	14,461
		H	V	80	14,385	18,370

HS-PSO: Harmony search-based particle swarm optimization, T.s: Roof drift, W: Frame weight, T.C: Total frame cost, V: Various.

11.2 Four bays with a ten-story frame.

Four bays with a ten-story frame is the second example. Fig. 21 shows the geometry of the frame, the member grouping and the design loads. The load values of W, W_1, and W_2 are 44.49 kN, 47.46 kN/m, and 42.91 kN/m, respectively. The member sections and story connections for the optimum solutions using BA and GA are shown in Tables 7 and 8, where as shown, the most rigid connections, i.e., types 6 and 7 are the most repeated, while connection type 5 is usually selected for top stories, moreover the most flexible connections, i.e., types 3 and 4 are chosen for middle stories.

Table 9 shows a comparison between the total frame cost of the optimum frame in the current study with those from previous studies, besides the frame weight and roof drift, while Figs. 22, 23 and 24 show the influence of base connection case on the roof drift, weight, and the total frame cost, respectively. As shown by the comparisons and figures, GA obtains better results than BA, while both of the algorithms reach better results than the literature results using the same base case, i.e., fixed base.

Moreover, there is an obvious relation between the base case and the total frame cost and weight, where the lowest cost and weight result in S case. On the other hand, H case results in the highest cost, weight, and roof drift.

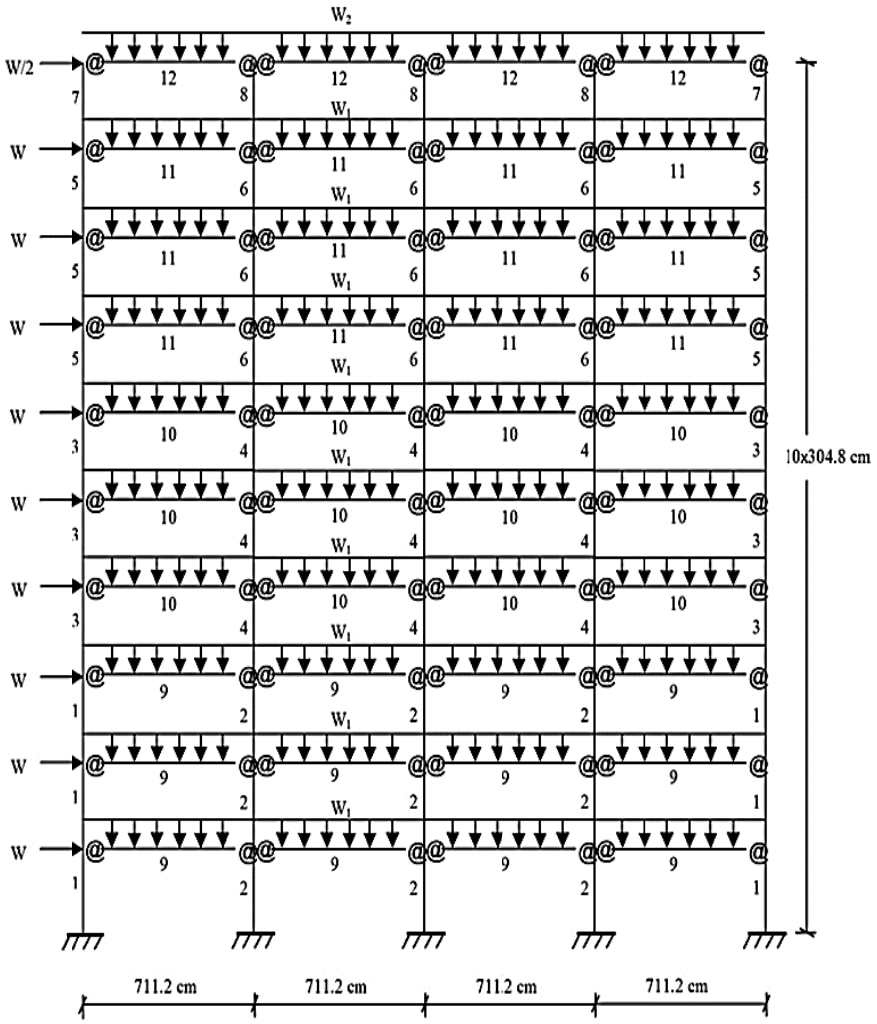

Fig. 21 Four bays with a ten-story frame [17]

Table 7 Member sections of optimum frames

Mem. Grouping no.	BA			GA		
	F	S	H	F	S	H
1	W30X90	W27X84	W24X76	W27X84	W27X84	W24X76
2	W36X135	W30X116	W38X149	W33X118	W33X118	W30X108
3	W24X55	W21X44	W24X76	W24X76	W21X50	W24X55
4	W27X84	W30X90	W30X116	W24X76	W24X76	W24X76
5	W21X44	W21X44	W24X68	W24X55	W21X50	W18X35
6	W21X44	W24X55	W24X62	W21X44	W21X44	W21X44
7	W21X44	W21X44	W24X68	W18X40	W18X35	W16X31
8	W21X44	W16X31	W16X31	W16X31	W16X31	W16X31
9	W21X44	W21X44	W24X68	W21X44	W21X44	W24X76
10	W24X55	W21X44	W18X40	W24X55	W21X50	W21X44
11	W18X35	W18X35	W18X35	W18X35	W18X35	W18X35
12	W16X31	W16X31	W16X31	W16X31	W16X31	W16X31

Table 8 Story connections of optimum frames.

Story no.	BA			GA		
	F	S	H	F	S	H
1	7	7	5	6	7	7
2	6	6	4	6	7	4
3	6	6	6	6	6	3
4	4	4	2	8	6	6
5	4	6	5	6	3	6
6	6	4	7	4	6	6
7	3	2	7	3	6	7
8	2	7	5	7	7	5
9	2	5	5	5	5	5
10	5	5	5	5	5	5

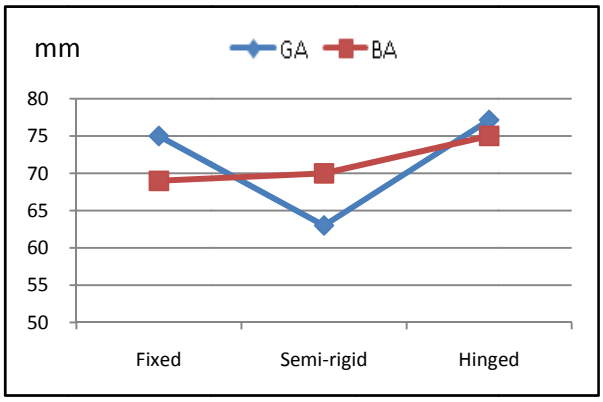

Fig.22 The roof drift using BA and GA

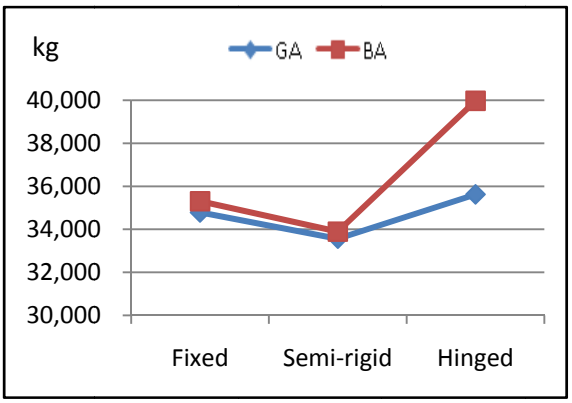

Fig.23 The total frame weight using BA and GA

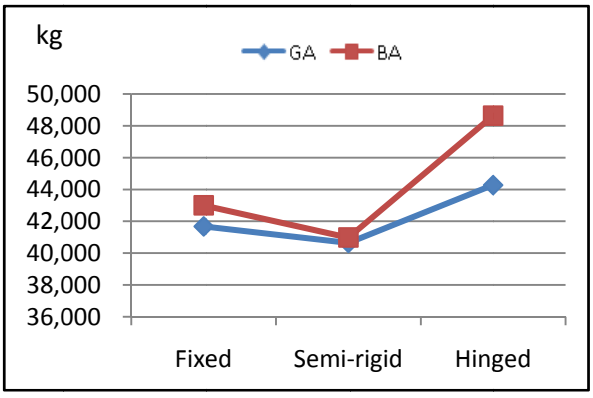

Fig. 24 The total frame cost using BA and GA

Table 9 Comparisons between the current study and previous works

Study	Algorithm	Base case	Conn.type	T.s (mm)	W (kg)	T.C (kg)
Rafiee et al. [22]	BB-BC	F	1	67	128,418	140,744
		F	2	25	195,578	237,050
		F	3	35	100,254	106,868
		F	4	58	87,432	93,255
		F	5	37	111,865	123,743
		F	6	40	103,357	113,055
		F	7	26	150,274	204,773
		F	8	56	126,120	136,881
Hadidi and Rafiee[21]	HS-PSO	F	1	76	52,196	58,939
		F	2	62	43,746	55,118
		F	3	58	40,040	46,328
		F	4	68	41,853	47,788
		F	5	63	38,532	46,407
		F	6	48	37,950	46,469
		F	7	49	38,737	47,328
		F	8	75	47,018	53,489
Hadidi and Rafiee[17]	BB-BC	F	V	41	114,133	120,891
	HS	F	V	55	50,772	60,691
	HS-BB-BC	F	V	68	38,115	44,343
Shallan et al. [1]	TLBO	F	V	68	34,507	41,827
	GA	F	V	75	34,786	41,676
Current study	GA	S	V	63	33,564	40,640
		H	V	77	35,624	44,276
	BA	F	V	69	35,308	43,000
		S	V	70	33,896	40,976
		H	V	75	39,975	48,640

11.3 Three bays with a twenty-four-story frame.

The third example is the 168-member frame. Its geometry, accompanied by the member grouping and design loads are shown in Fig. 25. The W, W_1, W_2, W_3, and W_4 loads have values of 25.628 kN, 4.378 kN/m, 6.362 kN/m, 6.917 kN/m, and 5.954 kN/m, respectively.

The story connections and member sections for the optimum solutions using BA and GA are shown in Tables 10 and 11, where as shown, the 3rd floor and above usually attains the most rigid connections, i.e., types 6 and 7, then, followed by more flexible connections, i.e., types 3, 4, and 8 till the most flexible connection, type 1, for the roof floor.

Table 12 presents a comparison between the total frame cost of the optimum frame in the current study with those from previous studies, along with the frame weight and roof drift. While Figs. 26, 27 and 28 display the effect of base connection case on the roof drift, weight, and the total frame cost, respectively. As shown from the comparisons and the figures, and similar to the previous examples, GA attains better results than BA, while both of the algorithms attain better results than the literature results using same base case, i.e., fixed base.

Furthermore, there is an apparent relation between the base case and the total frame cost and weight, whereas the lowest cost and weight are attained in S case. In contrast, the worst results, i.e., highest cost, weight, and roof drift result in H case.

Table 10 Story connections of optimum frames

Story no.	BA			GA		
	F	S	H	F	S	H
1,2	2	7	2	7	7	2
3,4	2	7	2	7	7	2
5,6	7	7	7	7	7	7
7,8	7	6	7	7	7	7
9,10	7	6	7	7	6	7
11,12	7	6	7	7	6	6
13,14	6	6	6	6	6	7
15,16	6	6	6	6	3	6
17,18	3	4	3	3	4	3
19,20	4	4	3	4	4	4
21,22	8	8	8	8	8	8
23,24	1	1	1	1	1	1

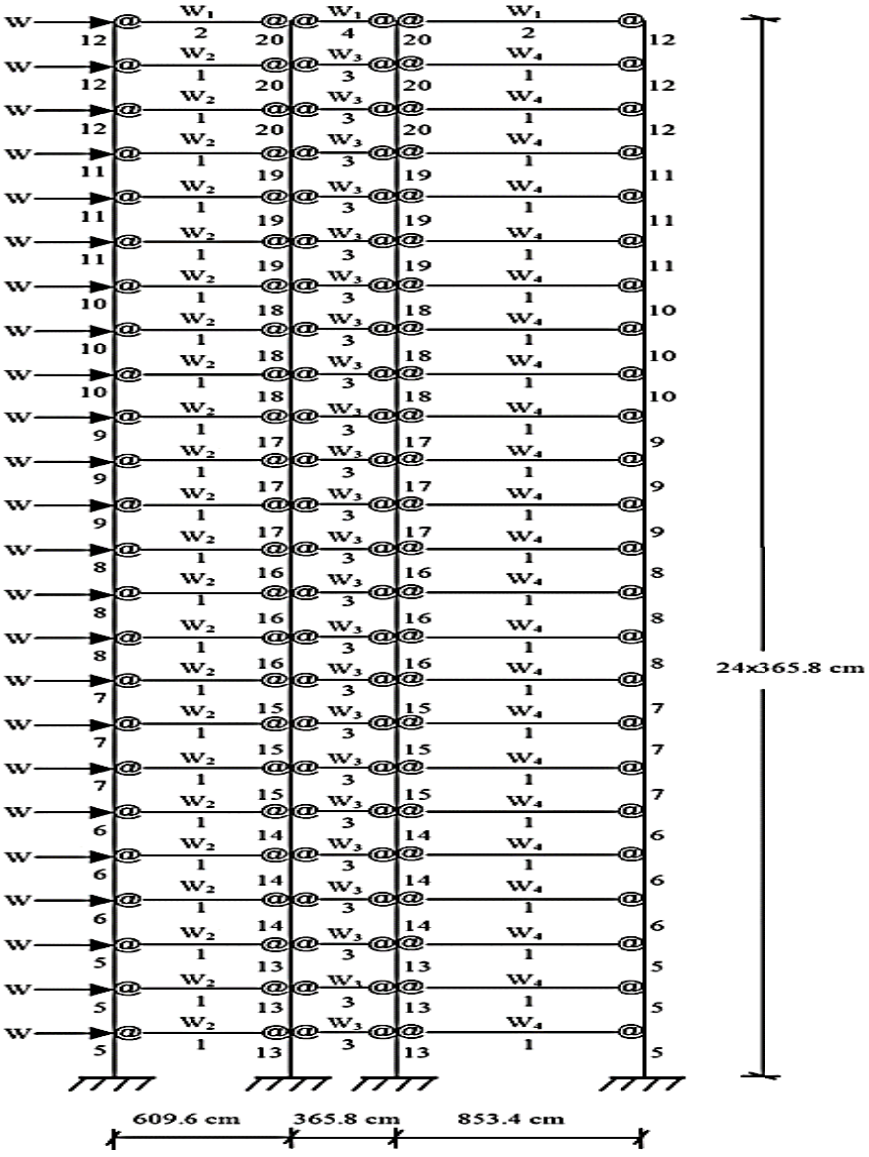

Fig. 25 Three bays with a twenty-four-story frame [17]

Table 11 Member sections of optimum frames

Mem. grouping no.	BA			GA		
	F	S	H	F	S	H
1	W24X68	W27X84	W24X68	W24X84	W27X84	W24X68
2	W12X14	W12X14	W16X31	W10X12	W10X12	W12X14
3	W30X90	W33X118	W30X116	W30X90	W24X76	W30X116
4	W8X10	W10X12	W12X14	W10X12	W8X10	W8X10
5	W33X130	W30X90	W39X167	W30X108	W33X118	W39X167
6	W33X130	W30X90	W39X167	W30X99	W33X118	W33X130
7	W33X118	W30X90	W38X149	W30X99	W30X116	W30X99
8	W30X116	W30X90	W30X90	W30X99	W30X90	W30X99
9	W24X68	W30X90	W30X90	W30X90	W27X84	W24X84
10	W24X68	W30X90	W27X84	W30X90	W27X84	W24X84
11	W24X68	W27X84	W27X84	W30X90	W27X84	W24X68
12	W24X68	W27X84	W24X68	W30X90	W27X84	W24X68
13	W38X149	W33X118	W43X230	W33X118	W33X118	W43X262
14	W38X149	W33X118	W33X130	W33X118	W30X90	W33X118
15	W38X149	W33X118	W33X130	W33X118	W30X90	W33X118
16	W38X149	W30X99	W30X90	W33X118	W30X90	W30X108
17	W38X149	W30X99	W30X90	W30X90	W27X84	W27X84
18	W38X149	W30X99	W30X90	W30X90	W27X84	W24X68
19	W30X99	W30X99	W24X84	W30X90	W27X84	W24X68
20	W30X99	W30X90	W24X84	W24X84	W27X84	W24X68

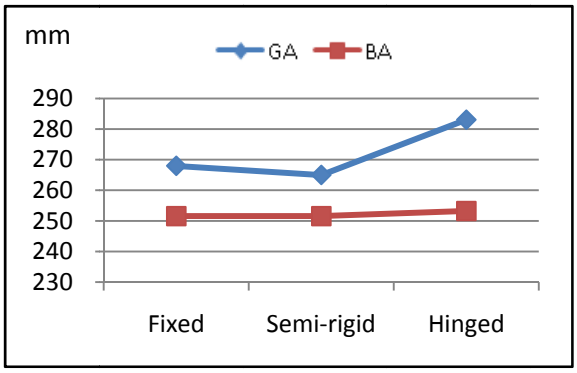

Fig. 26 The roof drift using BA and GA

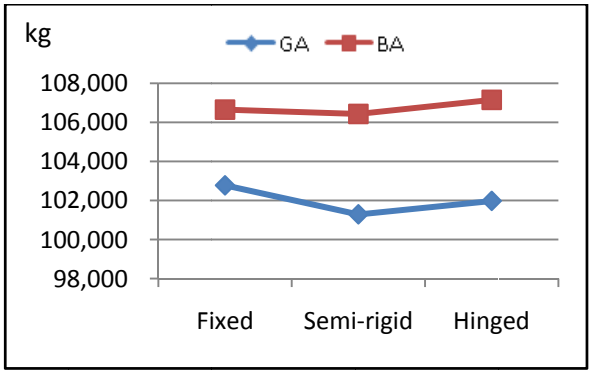

Fig. 27 The total frame weight using BA and GA

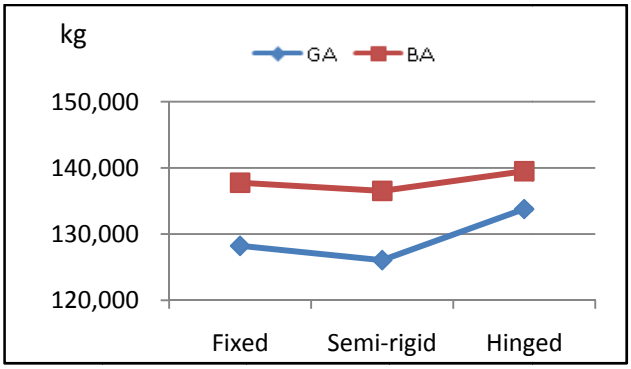

Fig. 28 The total frame cost using BA and GA

Table 12 Comparison between the current study and previous works

Study	Algorithm	Base case	Conn. type	T.s (mm)	W (kg)	T.C (kg)
Rafiee et al. [22]	BB-BC	F	1	204	381,754	502,197
		F	2	245	139,161	202,737
		F	3	170	236,249	267,414
		F	4	184	211,149	249,806
		F	5	237	140,536	171,868
		F	6	231	150,362	176,864
		F	7	240	359,372	385,074
		F	8	190	297,834	383,738
Hadidi and Rafiee[21]	HS-PSO	F	1	200	384,890	505,366
		F	2	245	135,368	189,791
		F	3	194	172,004	205,473
		F	4	208	175,521	210,296
		F	5	238	133,930	162,582
		F	6	217	137,054	165,828
		F	7	221	125,589	156,161
		F	8	203	261,722	341,798
Hadidi and Rafiee[17]	BB-BC	F	V	212	238,721	260,152
	HS	F	V	174	209,040	289,580
	HS-BB-BC	F	V	255	132,313	151,481
Shallan et al. [1]	TLBO	F	V	263	105,550	131,322
	GA	F	V	268	102,778	128,226
Current study	GA	S	V	265	101,289	126,065
		H	V	283	101,977	133,795
	BA	F	V	252	106,657	137,764
		S	V	252	106,435	136,530
		H	V	253	107,156	139,508

XII. CONCLUSIONS

Accurate simulation of semi-rigid beam-to-column connections, along with semi-rigid base connections is very significant to attain accurate results for frame response. This study attempts to make an optimization for semi-rigid frames, whereas semi-rigid beam-to-column and base connections are simulated using logical Frye and Morris and Kanvindemodels, respectively. The current study is applied to three benchmark problems using two of the best optimization algorithms, BA and GA, and the following results are obtained.

- There is a noticeable relationship between the base case with the cost and weight of the frame, where, semi-rigid base case produces the lowest cost and weight in comparison with fixed and hinged base cases.
- Conversely, hinge base case results in the highestcost, weight, and roof drift.
- For the distribution of beam-to-column connections types through frame floors, the distribution mostly begins with the stiffest types for lower floors and as the floors get higher as they get more flexible types.
- More obviously shown by the results, GA attains better results than BA for all examples and for all base cases.

XIII. REFERENCES

[1] O. Shallan, H. M. Maaly, and O. Hamdy, "A developed design optimization model for semi-rigid steel frames using teaching-learning-based optimization and genetic algorithms," Struct. Eng. Mech., vol. 2, pp. 173–183, 2018.
[2] A. M. Kanvinde, D. A. Grilli, and F. Zareian, "Rotational Stiffness of Exposed Column Base Connections: Experiments and Analytical Models," J. Struct. Eng., vol. 138, no. 5, pp. 549–560, 2012.
[3] M. J. Frye and G. A. Morris, "Analysis of Flexibly Connected Steel Frames," Can. J. Civ. Eng., vol. 2, no. 3, pp. 280–291, 1975.
[4] American Institute of Steel Construction, ANSI/AISC 360-16. Specification for Structural Steel Buildings. 2016.
[5] K. M. Abdalla and W. F. Chen, "Expanded database of semi-rigid steel connections," Comput. Struct., vol. 56, no. 4, pp. 553–564, 1995.
[6] M. L. Chisala, "Modelling M-φ curves for standard beam-to-column connections," Eng. Struct., vol. 21, no. 12, pp. 1066–1075, 1999.
[7] J. H. Kim, J. Ghaboussi, and A. S. Elnashai, "Mechanical and informational modeling of steel beam-to-column connections," Eng. Struct., vol. 32, no. 2, pp. 449–458, 2010.
[8] Z. Wu, S. Zhang, and S. F. Jiang, "Simulation of tensile bolts in finite element modeling of semi-rigid beam-to-column connections," Int. J.

Steel Struct., vol. 12, no. 3, pp. 339–350, 2012.
[9] A. C. Aydin, M. Kiliç, M. Maali, and M. Saɨiroɨlu, "Experimental assessment of the semi-rigid connections behavior with angles and stiffeners," J. Constr. Steel Res., vol. 114, pp. 338–348, 2015.
[10] M. Maali, M. Kılıç, M. Sağıroğlu, and A. C. Aydın, "Experimental model for predicting the semi-rigid connections' behaviour with angles and stiffeners," Adv. Struct. Eng., vol. 20, no. 6, pp. 884–895, 2017.
[11] J. S. Hensman and D. A. Nethercot, "Numerical study of unbraced composite frames: Generation of data to validate use of the wind moment method of design," J. Constr. Steel Res., vol. 57, no. 7, pp. 791–809, 2001.
[12] M. Artar and A. T. Daloglu, "Optimum weight design of steel space frames with semi-rigid connections using harmony search and genetic algorithms," Neural Computing and Applications, pp. 1–12, 2016.
[13] M. Artar, "Optimum design of braced steel frames via teaching learning based optimization," Struct. Eng. Mech., vol. 22, pp. 733–744, 2016.
[14] M. Artar and A. T. Daloɨlu, "Optimum design of composite steel frames with semi-rigid connections and column bases via genetic algorithm," Steel Compos. Struct., vol. 19, no. 4, pp. 1035–1053, 2015.
[15] M. Artar and A. Daloglu, Optimum design of steel frames with semi-rigid connections and composite beams, vol. 55. 2015.
[16] M. Artar and A. Daloglu, Optimum design of steel space frames with composite beams using genetic algorithm, vol. 19. 2015.
[17] A. Hadidi and A. Rafiee, "A new hybrid algorithm for simultaneous size and semi-rigid connection type optimization of steel frames," Int. J. Steel Struct., vol. 15, no. 1, pp. 89–102, 2015.
[18] M. Yassami and P. Ashtari, "Using fuzzy genetic algorithm for the weight optimization of steel frames with semi-rigid connections," Int. J. Steel Struct., vol. 15, no. 1, pp. 63–73, 2015.
[19] M. Alqedra, A. Khalifa, and M. Arafa, "An Intelligent Tuned Harmony Search Algorithm for Optimum Design of Steel Framed Structures to AISC-LRFD," Adv. Res., vol. 4, no. 6, pp. 421–440, 2015.
[20] M. Arafa, A. Khalifa, and M. Alqedra, "Design Optimization of Semi - Rigidly Connected Steel Frames Using Harmony Search Algorithm," MSc. Dissertation ,Gaza University, 2011.
[21] A. Hadidi and A. Rafiee, "Harmony search based, improved Particle Swarm Optimizer for minimum cost design of semi-rigid steel frames," Struct. Eng. Mech., vol. 50, no. 3, pp. 323–347, 2014.
[22] A. Rafiee, A., Talatahari, S., and Hadidi, "Optimum design of steel frames with semi-rigid connections using big bang-big crunch method," Steel Compos. Struct., vol. 14, no. 5, pp. 431–451, 2013.
[23] S. O. Degertekin and M. S. Hayalioglu, "Harmony search algorithm for minimum cost design of steel frames with semi-rigid connections and column bases," Struct. Multidiscip. Optim., vol. 42, no. 5, pp. 755–768, 2010.
[24] M. S. Hayalioglu and S. O. Degertekin, "Minimum cost design of steel frames with semi-rigid connections and column bases via genetic optimization," Comput. Struct., vol. 83, pp. 1849–1863, 2005.
[25] M. S. Hayalioglu and S. O. Degertekin, "Design of non-linear steel frames for stress and displacement constraints with semi-rigid connections via genetic optimization," Struct. Multidiscip. Optim., vol. 27, no. 4, pp. 259–271, 2004.
[26] S. O. Degertekin and M. S. Hayalioglu, "Design of non-linear semi-rigid steel frames with semi-rigid column bases," Electron. J. Struct. Eng., vol. 4, no. October, pp. 1–16, 2004.
[27] D. E. Goldberg and J. H. Holland, "Genetic Algorithms and Machine Learning," Machine Learning, vol. 3, no. 2, pp. 95–99, 1988.
[28] D. T. Pham, A. Ghanbarzadeh, E. Koc, S. Otri, S. Rahim, and M. Zaidi, "Bee Algorithm A Novel Approach to Function Optimisation," Manuf. Eng. Cent., vol. 501, no. September, 2005.
[29] B. S. Dhillon and J. W. O'Malley III, "Interactive Design of Semirigid Steel Frames," Journal of Structural Engineering, vol. 125, no. 5. pp. 556–564, 1999.
[30] A. Chajes and J. E. Churchill, "Nonlinear Frame Analysis by Finite Element Methods," J. Struct. Eng., vol. 113, no. 6, pp. 1221–1235, 1987.
[31] L. Xu and D. E. Grierson, "Computer Automated Design of Semirigid Steel Frameworks," J. Struct. Eng., vol. 119, no. 6, pp. 1740–1760, 1993.